30TH INTERNATIONAL COSMIC RAY CONFERENCE

Effect of the improved data acquisition system of IceCube on its neutrino-detection capabilities

DMITRY CHIRKIN[1] FOR THE ICECUBE COLLABORATION[2]
[1]*Lawrence Berkeley National Laboratory, Berkeley, CA, U.S.A.*
[2]*see special section of these proceedings*
dchirkin@lbl.gov

Abstract: The IceCube data acquisition system is capable of recording information about all photons registered by its photomultiplier tubes for up to 13 microseconds for each sensor with high precision. A time resolution of 3 ns and charge resolution of 30% of all one photoelecton pulses within each sensor's event record is achieved. The improvement in quality of the data reconstruction due to the improved design of the experiment is estimated and its effect on the IceCube capabilities as a neutrino detector is discussed.

Introduction

The ability of IceCube optical sensors to record information about all photon registered by their PMTs has not yet been fully utilized in the data analysis (see, e.g., [1]). While the much improved timing and energy resolution are being used to improve upon the energy resolution of the detected muon events [2], this contribution attempts to demonstrate the improvement in muon neutrino analysis due to the ability to separately detect individual photoelectrons with their respective times and charges (shown in Figure 1).

The goal of selecting muon neutrinos in the presence of a 10^6 times higher background of atmospheric muons is to maximize the signal yield at a low background level, while achieving the best possible resolution with least mis-reconstruction of signal events.

In this preliminary study we present the analysis of one month of data collected by a 9-string IceCube detector configuration in year 2006. Data reconstruction algorithms using only the first photon per sensor were compared with those incorporating the full multi-photon information. The angular resolution achieved in both cases is very similar; however, the number of badly mis-reconstructed signal events is lower for multi-photon reconstruction. Using the additional information available from all

recorded photons leads to the correspondingly improved separation of signal and background and allows one to to achieve the required background reduction while retaining a higher signal yield.
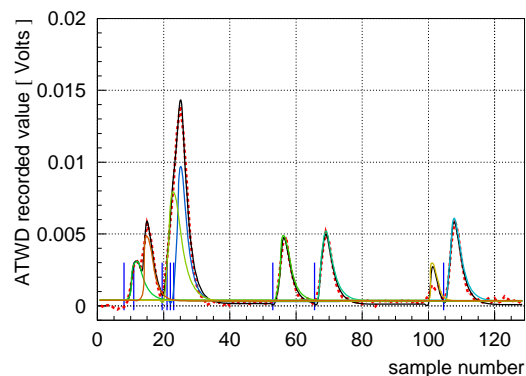

Figure 1: A typical PMT signal trace recorded by the faster digitizer of an IceCube optical sensor. The trace contains 128 samples, 3.3 ns. per sample. Results of 2 different photon deconvolution methods shown agree well. Blue vertical lines denote the hit times of the first method. The black fit line with colored lines denote deconvolved pulses of the second method. The data is shown with a red dashed line.
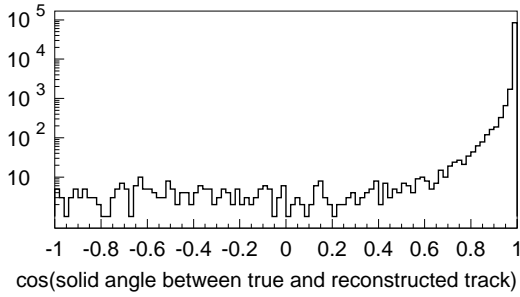
Figure 2: Distribution of the deviation of the reconstructed from the true direction for the studied simulated data sample shown after some cuts.

A new method of combining cuts to optimize background reduction is presented. First, a robust definition of angular resolution of reconstructed muon direction in simulated data is introduced. The cuts are optimized to maximize the angular resolution of the remaining events, and then are tightened to remove the background of misreconstructed events.

Angular resolution and cut optimization

The precision of the track reconstruction methods is determined from the deviation of the reconstructed result from the true track direction from the simulation (typical distribution shown in Figure 2). It was not possible to describe all such distributions at different reconstruction quality levels with a single shape depending only on the distribution width. Therefore the following very general definition was introduced instead: the *angular resolution* α of a given simulated data sample is chosen so that 2/3 of the data have reconstructed result deviate from the true track direction by less than the resolution, and 1/3 by more. This simple definition allows one to calculate the angular resolution α easily for all data quality levels, providing a good measure of the effectiveness of the quality cuts.

The cut parameters were chosen to have the following property: as the value of the cut on the parameter is lowered (i.e., the cut becomes stronger), the angular resolution α, as defined above, improves.

Several reconstructions were performed in succession. These differed by the ice description used in the calculation of the photon scattering probabilities, by whether the muon energy was allowed to vary during the reconstruction, and whether all recorded photons or only first recorded photons were used.

For each reconstruction several quantities have the "cut property" defined above: minus reduced log likelihood of the reconstructed result, closest approach distance from the reconstructed track to the center of gravity of hits, relative uncertainty and variation of the energy measure, and uncertainty in the zenith and azimuth angles (defined as the range in the parameter in which the log likelihood stays above its maximum minus 0.5). Additionally the differences in the direction of different reconstruction results were formed. One more parameter appeared necessary: 1 over the total length of the track defined as the distance between two farthest from each other projections of hits on the reconstructed track. Parameters with similar distributions were grouped together, resulting in 7 groups. In each group the maximum value of the parameters in the group was chosen as the parameter of the group.

Cuts c_i, $i = 1, ..., 7$ were applied to the parameter groups defined above in such a way as to maximize the angular resolution α for each given fraction of events r left after the cuts. The fastest decent approach was chosen to optimize the cuts: starting with a full dataset, at each step reducing the fraction of the events left by the amount δr the cuts were adjusted by the amount proportional to $\partial \alpha / \partial c_i$.

Since the relative and overall cut strength depends on the number of degrees of freedom available during the reconstruction, cuts were optimized individually for event groups with different number of sensors with signal (here called channels) N_{ch} from the simulated dataset. This resulted in a set of cuts, one representation of which, describing achievable efficiencies (fractions of events left, r_n) for given α and N_{ch}, here called *efficiency matrix*, is shown in Figure 3. In order to determine the cut sets needed to achieve a certain angular resolution α the efficiency matrix is consulted to determine the fractions of events r_n with given $n = N_{ch}$. The set of cuts strong enough to leave only a frac-
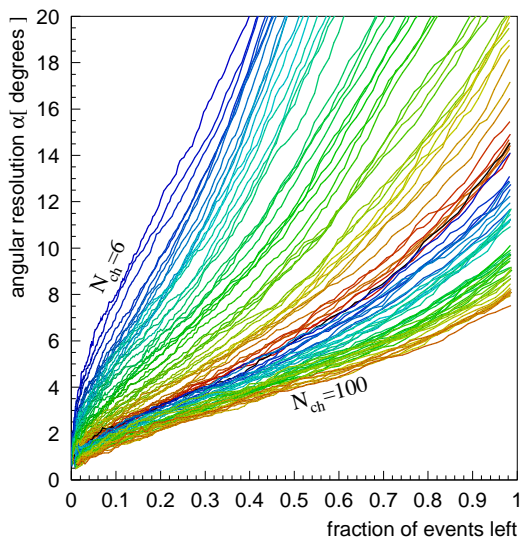
Figure 3: Efficiency matrix shows for each N_{ch} the best achievable angular resolution α at each given fraction of events left after applying cuts (this definition is equivalent to that given in the text).

tion r_n of events that were used in the efficiency matrix evaluation are then the cuts that reduce the data to a set with the desired angular resolution α.

To study the improvement in data analysis due to the availability of information about multiple pulses from each sensor the parameters corresponding to the multi-photon reconstructions were removed from the cut groups defined above. The resulting efficiency matrix looks nearly identical to the one shown in Figure 3 except that points on the lines correspond to somewhat more constrained cut values as compared to the multi-photon-enabled efficiency matrix. Therefore the first-photon-only cuts are just as effective as the complete cut set in improving the angular resolution α for a given data reduction fraction. This, however, is to be expected for a self-sufficient cut set, meaning that more cuts do not improve the angular resolution for a given fraction with the used angular resolution definition.

Nevertheless, as shown in the following section, at the final neutrino selection cut levels there is a substantial improvement in both the angular resolution α of the final sample and the fraction of events retained, indicating that the outliers of the angular distribution are reduced in the analysis employing
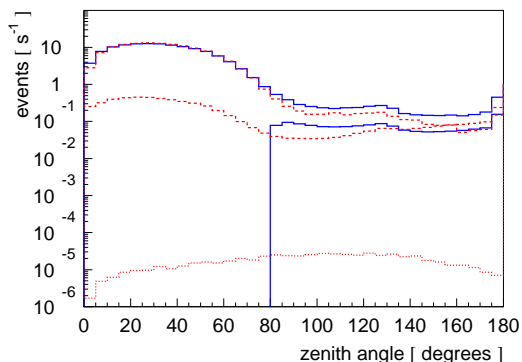

Figure 4: Initial zenith angle distribution (no cuts): red dashed lines: upper: downgoing muon background, lower: coincident downgoing shower background; red dotted line: muons from atmospheric muon neutrinos; upper blue line: reconstructed data; lower blue line: reconstructed data with cut of zenith angle above 80 degrees applied to all reconstructions.

the full cut set, showing the clear advantage of the method utilizing all recorded pulses.

Atmospheric neutrino search

Figure 4 shows the zenith angle distribution of reconstructed tracks in real and simulated data. The data remaining after the cuts on the zenith angle for all reconstructions are applied contains mostly poorly reconstructed downgoing background events that fall into the tail of events reconstructed with wrong direction shown in Figure 2. The data shown in Figure 2 is at the cut level corresponding to an angular resolution α of 4 degrees; misreconstructed events are suppressed by more than 4 orders of magnitude at this cut level. Without any cuts the level of misreconstructed events is higher, about 2 orders of magnitude below the peak, matching the level of misreconstructed events in Figure 4. By applying successively stronger cuts corresponding to lower values of angular resolution α the background of misreconstructed events can be reduced until most of the events reconstructed as upgoing are, indeed, upgoing.

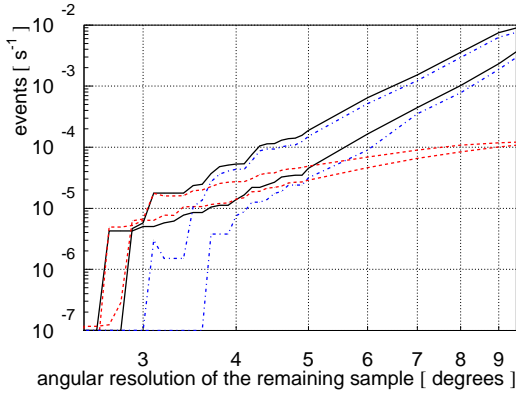To determine the angular resolution α required to suppress the background of misreconstructed

Figure 5: Events remaining at different cut levels corresponding to requested values of angular resolution α. Black solid: data; red dashed: muon neutrino simulation; blue dashed-dotted: background simulation. Upper curves are for full cut set; lower curves are for first-photon-only cut set.
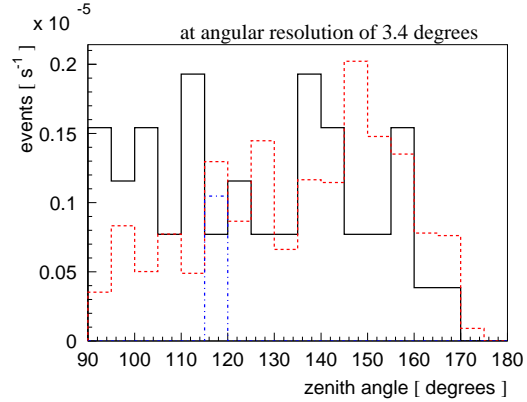

Figure 6: Zenith angle distribution at final cut level. Black solid line: data; red dashed: muon neutrino simulation; blue dashed-dotted: one event remaining from the background simulation.

events below the signal of upgoing events successively stronger cuts are applied. At each cut level the data left after the cuts is compared to simulation of both background and signal, as shown in Figure 5. The cut level required to achieve the desired signal purity can thus be selected. The 50% purity is achieved at the intersection points of simulated background and neutrino lines in Figure 5: at angular resolution α=3.7 with 96 events left for the full cut set, and at angular resolution α=4.9 degrees with 90 events left for the first-photon-only data set. At the same signal purity level the angular resolution α of neutrino events in the remaining sample is 30% better for the full set.

It is more difficult to estimate the purity and number of events left as the cuts are tightened more, due to the limited amount of simulated data at the time this paper was written. However, following the lines of Figure 5, one could estimate the angular resolution α and number of events left at $\sim$ 90% purity level of 3.4 degrees and 46 events (shown in Figure 6) for the full cut set, and 3.6 degrees and 22 events for the first-photon-only cut set. This indicates that at the highest signal purity levels the number of neutrino events is more than doubled when incorporating the full information about all pulses into the analysis.

Conclusions

A new approach to background rejection in Ice-Cube is taken: instead of optimizing cuts to maximize signal over background, cuts are first optimized to maximize the angular resolution α of single muon tracks while retaining as many of the events as possible. Then the cuts corresponding to successively better values of angular resolution α are applied until the desired signal purity is achieved.

This approach allowed us to study the effect of including the complete information on all pulses recorded by the optical sensors of the detector. The number of signal events retained at the highest purity levels doubled (important for diffuse analysis), while the angular resolution α at somewhat relaxed cuts improved by 30 %.

References

[1] Pretz, J. for the IceCube Collaboration, these proceedings
[2] Zornoza, J. for the IceCube Collaboration, these proceedings
[3] Karle, A., these proceedings